Fermentable Dietary Fiber Potentiates the Localization of Immune Cells in the Rat Large Intestinal Crypts

SATOSHI ISHIZUKA,[1] SEIJI TANAKA, HONG XU, AND HIROSHI HARA
Division of Applied Bioscience, Graduate School of Agriculture, Hokkaido University, Sapporo 060-8589, Japan

Intestinal crypts are composed of a well-defined hierarchy of epithelial cells, and proliferating epithelial cells reside close to the bottom of the crypts—even in the large intestine. We investigated whether $CD8^+$ and $CD4^+$ intraepithelial lymphocytes (IELs) and $CD161^+$ natural killer (NK) cells localized in proliferating or differentiated epithelial region of cecum and colon. Both proliferating epithelial layer cells and the immune cells along the longitudinal crypt axis of the large intestine were measured histochemically. Dietary intervention revealed that the physiological localization of the immune cells in the longitudinal crypt axis depended on the immune cell type. $CD8^+$ IELs were preferentially located among differentiated epithelial cells. In contrast, $CD161^+$ NK cells were located adjacent to the epithelial cells at the bottom of crypt. Cecal crypts contained significantly larger numbers of $CD8^+$ IELs than did colonic crypts. However, there was only a minor population of $CD4^+$ IEL in the cecal and colonic epithelia. Some dietary fibers increased the densities of $CD8^+$ IELs and $CD161^+$ NK cells in the cecum, with the magnitude of response varying among the types of fiber. There was a significant relationship between SCFA and the localization of immune cells, especially $CD8^+$ IEL and $CD161^+$ NK cells, which are considered to be involved in the maintenance of epithelial homeostasis. Exp Biol Med 229:876–884, 2004

Keywords: crypt; dietary fiber; $CD161^+$ natural killer cell; $CD8^+$ intraepithelial lymphocytes

This work was supported in part by a grant from Japan Society for the Promotion of Science.

[1] To whom requests for reprints should be addressed at Division of Applied Bioscience, Graduate School of Agriculture, Hokkaido University, Sapporo 060-8589, Japan. E-mail: zuka@chem.agr.hokudai.ac.jp

Received December 12, 2003.
Accepted June 7, 2004.

1535-3702/04/2299-0876$15.00

Introduction

Intraepithelial lymphocytes (IELs) play a significant role in epithelial homeostasis. For example, abrogation of gammadelta IELs reduces epithelial cell turnover (1) and enhances azoxymethane-induced colorectal carcinogenesis and aberrant crypt foci (2), which are a preneoplastic biomarker for colorectal carcinogenesis (3). To investigate the relationship between colorectal carcinogenesis and the immune system, we focused on the large intestine and found that a reduction in $CD8^+$ IELs by treatment with anti-asialo GM1 is accompanied by an increase in the number of aberrant crypts in the colorectum and that ingestion of sugar beet fiber (SBF) partially restores the number of $CD8^+$ IELs in the colonic epthelium (4). Thus, the accumulation of $CD8^+$ IELs is modified by dietary intervention. Cytotoxicity mediated by natural killer (NK) cells is considered to play an important role in anticancer defense mechanisms (5). Recently, the $CD3^-NKR\text{-}P1^+$ ($CD161^+$) subset was found in the isolated IEL fraction from the rat small intestine, and the $CD161^+$ cells were found to have strong NK activity (6, 7). The $CD161^+$ NK cells may play a role in mucosal immune surveillance; nevertheless, there is very little information regarding the physiological localization of these immune cells around the crypt.

The intestinal epithelium is a highly proliferative, hierarchical organ in which stem cell position is well defined in terms of the spatial arrangement, even within the large intestinal crypt (8). Potten and colleagues extensively studied the spatial distribution of epithelial cells that undergo apoptosis, mitosis, proliferation, and expression of p53 and p21 protein along the longitudinal crypt axis of the intestinal epithelium. In general, proliferating epithelial cells reside close to the bottom of the crypt. Primarily $CD8^+$ IELs are scattered among the epithelial cells, but their distribution is not well defined along the longitudinal crypt axis. A spatial arrangement of immune cells along the longitudinal crypt axis should be observed, as with the proliferating epithelial cells, if the localization of the immune cells is important for epithelial homeostasis.

Dietary intervention may influence such localization of immune cells in a physiological condition.

Microbiota affect not only host mammalian nutritional status (9) but also interaction between epithelia and IELs (10). *Bacterides thetaiotaomicron* in the luminal contents induces angiogenesis in the intestinal villi in a gnotobiotic study (11), and it is widely accepted that ingesting dietary fiber changes the concentration of organic acids in luminal contents of the large intestine (12). Some dietary fibers have the ability to promote production of such organic acids in the luminal contents, and the fermentation profile depends on the source of the dietary fiber ingested. Of these organic acids, short-chain fatty acids (SCFAs) are known to affect the large intestine. For instance, butyrate is used as a primary energy source in colonic epithelial cells (13, 14) and stimulates normal epithelial cell proliferation (15). Indeed, we demonstrated that ingestion of SBF, a fermentable fiber, promotes a greater physiological accumulation of $CD8^+$ IELs in the crypts of the rat large intestine than does relatively unfermentable fiber (16). The $CD8^+$ IEL population is greatest in the cecal mucosa and gradually declines toward the distal large intestine.

In this study, we applied cell-positional analysis, which was originally established for epithelial cells (8), to the distribution of immune cells to evaluate the physiological localization of IELs and NK cells along the longitudinal crypt axis in the rat large intestine. Furthermore, we analyzed whether ingestion of dietary fiber modulates the density and distribution of IELs and NK cells on a cell-position basis in the crypt, accompanied with SCFA analysis of the cecal contents.

Materials and Methods

Animals and Diets. This study was approved by the Hokkaido University Animal Use Committee, and the animals were maintained under the guidelines of Hokkaido University for the care and use of laboratory animals. Thirty male WKAH/HkmSlc rats (5 weeks old, Japan SLC) were housed in individual cages in a temperature-controlled room under a 12-hour photoperiod (light: 0800–2000 hours). The fiber-free (FF) diet contained sucrose, casein, corn oil, choline bitartrate, a mineral mixture, and a vitamin mixture according to AIN-93 formulation (17, 18). Rats were allowed free access to food and water over the experimental period. All rats were fed the FF diet for 7 days. After the acclimation period, they were divided into 5 dietary groups fed FF or dietary fiber (50 g/kg diet)–containing diets at the expense of sucrose. The dietary fibers used in this experiment were as follows: cellulose (CE; microcrystalline cellulose PH-102, Asahi Kasei Co.), SBF (Nippon Beet Sugar MFG), guar-gum hydrolysate (GGH; Meiji Seika Kaisha Ltd.), and water-soluble soybean fiber (WSF; Fuji Oil Co.). After 3 weeks of feeding the rats with the test diets, the rats were sacrificed (at 1000–1300 hours) by decapitation under anesthesia with diethylether, and the cecum and distal colon were removed. Rats were injected with bromodeoxyuridine (BrdU) solution at 1 h before the sacrifice, as previously reported (19). Segments of the large intestine (cecum and distal colon) were flushed with saline, embedded into Optimal Cutting Temperature compound (Sakura Finetechnical Co., Ltd.) in liquid nitrogen, and frozen at –80°C. The cecal contents were stored at –40°C until analysis.

Immunohistochemical Analysis. Antibodies used in this study were as follows: mouse anti-CD4 (clone W3/25, Serotec), mouse anti-CD8 (clone OX-8, Cedarlane), mouse anti-NKR-P1 (CD161; clone 10-78, Cederlane), and anti-BrdU (clone OS94.6, Calbiochem). Frozen sections from these samples were fixed at 4°C with Zamboni's fixative for CD4 and CD8 staining or with periodate-lysine-paraformaldehyde for CD161 detection (16). After being fixed, these sections were immersed in 3% hydrogen peroxide in methanol to reduce endogenous peroxidase activity. They were incubated for 1 hour with 10% normal rabbit serum to block nonspecific bindings. After incubation with the primary antibody, sections were incubated with rabbit anti-mouse IgG conjugated with biotin. They were then incubated with peroxidase-conjugated streptavidin. For the chromogen, we used 3,3′-diaminobenzidine tetrahydrochloride. All sections were counterstained with hematoxylin. To verify the specificity of the signals produced, we confirmed the negative control by omission of each primary antibody, but with inclusion of all the other steps and reagents. The number of $CD4^+$, $CD8^+$, $CD161^+$, and $BrdU^+$ cells in the epithelial layer cells (epithelial cells and adjacent to the epithelial cells) in the well-shaped crypt section was scored for 50 half crypts in each part of the large intestine. Cell position means the location of certain epithelial cells from the bottom in the well-shaped crypt section. We then calculated the ratio of $CD4^+$, $CD8^+$, and $CD161^+$ cells against 100 epithelial layer cells and the number of these immune cells located at cell positions 1–17 and >17.

Organic Acid Concentration in Cecal Contents. The concentration of organic acids (succinate, lactate, acetate, propoinate, iso-butyrate, butyrate, iso-valerate, and valerate) in the cecal contents was measured by ion-exclusion chromatography using a high-performance liquid chromatography system equipped with a solvent delivery system (SCL-10AVP, Shimadzu), a double ion-exchange column (Shim-pack SCR-102H, 8 x 300 mm, Shimadzu), and an electroconductivity detector (CDD-6A, Shimadzu) according to the method of Hoshi *et al.* (20). Briefly, sodium hydroxide aqueous solution containing crotonic acid as an internal standard was added to the cecal contents. After centrifugation, the fat-soluble substance in the supernatant was removed by extraction with chloroform. The aqueous phase was filtered through a membrane filter and applied to high-performance liquid chromatography. The mobile phase consisted of 5 m*M* *p*-toluenesulfonic acid.

Statistical Analysis. All results are expressed as means ± SEM. The data were analyzed by two-way ANOVA (site and diet) for distribution of $BrdU^+$ epithelial cells. Statistical comparisons among dietary groups were performed using Tukey-Kramer's test at $P < 0.05$. The number of IELs and NK cells between the lower (1–17) and upper (>17) cell positions in crypts was analyzed by Student's *t*-test at $P < 0.05$. We also analyzed linear regression using the least squares method between the number of immune cells and concentration of each organic acid, and the number of $CD8^+$ IELs at cell position >17 and the number of $CD161^+$ NK cells at cell positions 1–17.

Results

Representative Immunohistochemistry of $BrdU^+$ Epithelial Cells, $CD8^+$IEL, $CD4^+$IEL, and $CD161^+$ NK Cells Around the Large Intestinal Crypt. There were no significant differences in final body weight after the experimental period regardless of the dietary fiber ingestion. Figure 1 shows representative photographs of $BrdU^+$ (Fig. 1A), $CD8^+$ (Fig. 1B), $CD4^+$ (Fig. 1C), and $CD161^+$ (Fig. 1D) cells in the rat large intestine. Many $BrdU^+$ epithelial cells and $CD8^+$ IELs were observed in the mucosa. In contrast, the number of $CD4^+$ IELs was very low, although $CD4^+$ cells were often observed in the lamina propria. $CD161^+$ cells appeared to locate both in the lamina propria and adjacent to the epithelial cells near the crypt bottom. In this study, we scored the $CD161^+$ NK cells as epithelial layer cells like $CD8^+$ or $CD4^+$ IELs. $CD8^+$ IELs were observed mainly near differentiated epithelial cells of the crypts. No pathological accumulation of immune cells was observed in all rats.

Frequency of $CD8^+$ IELs, $CD4^+$ IELs, and $CD161^+$ NK Cells in Cecal and Colonic Crypt Epithelium. Scoring of $CD8^+$ IELs (Fig. 2A), $CD4^+$ IELs (Fig. 2B), and $CD161^+$ NK cells (Fig. 2C) along with the epithelial layer cells showed that the number of $CD8^+$ IELs per 100 epithelial layer cells was basically greater in cecal crypts than in the crypts of the distal colon. Ingestion of dietary fiber significantly promoted accumulation of the $CD8^+$ IELs into the cecal epithelium. The ratio of $CD161^+$ NK cells in the cecum of SBF-fed rats was significantly larger than that of the CE-fed rats (Fig. 2C). In contrast, almost no apparent change in the number of $CD4^+$ IELs was observed regardless of dietary fiber ingestion, although the number tended to increase toward the distal colon.

Proliferation of Epithelial Cells in the Cecal and Colonic Crypt. Figure 3 shows BrdU incorporation in the epithelial layer cells of the cecum (Fig. 3A) and distal colon

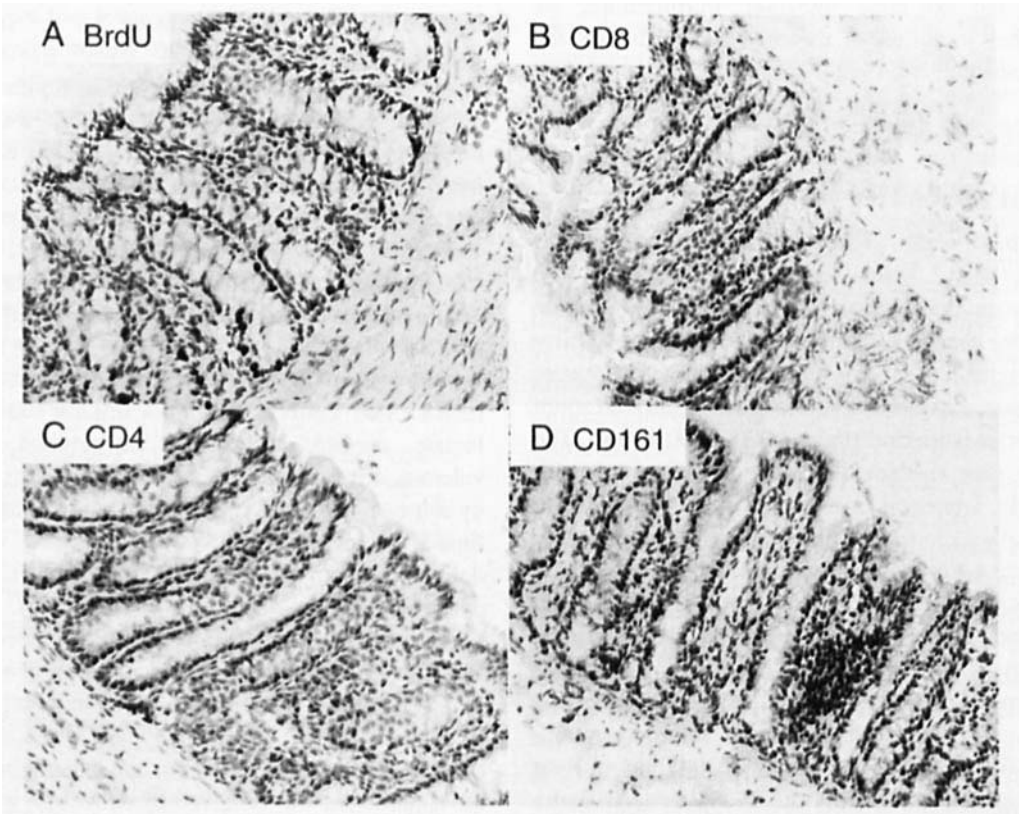

Figure 1. Representative photographs showing $BrdU^+$ epithelial cells, $CD8^+$ intraepithelial lymphocytes, $CD4^+$ intraepithelial lymphocytes, and $CD161^+$ natural killer cells in the rat large intestinal crypt. $BrdU^+$ epithelial cells located at the bottom of the crypt (A). In contrast, $CD8^+$ intraepithelial lymphocytes are located in the upper region of the lamina propria and the intraepithelial region (B). Very few $CD4^+$ intraepithelial lymphocytes were found (C). A certain number of $CD161^+$ natural killer cells were observed in the lamina propria, and some $CD161^+$ natural killer cells were located adjacent to the epithelial cells in the bottom of the crypt; natural killer clusters are also often observed (D).

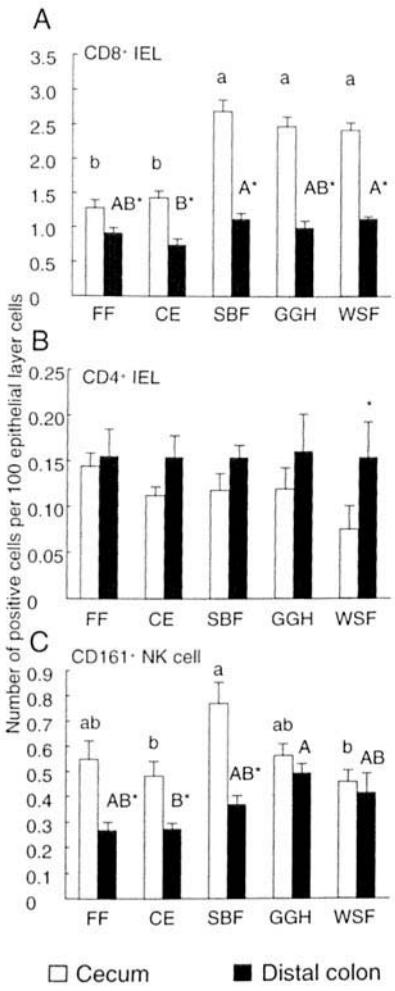

Figure 2. Number of $CD8^+$ (A) and $CD4^+$ (B) intraepithelial lymphocytes, and $CD161^+$ natural killer cells (C) per 100 epithelial layer cells in the half-crypt section in cecal (open bars) and distal colonic (filled bars) crypts of rats fed various dietary fibers. The data were shown as the means ± SEMs (n = 6). Bars with different small letters show significant differences ($P < 0.05$) in the cecum among dietary groups. Bars with different capital letters show significant differences ($P < 0.05$) in the distal colon among dietary groups. Asterisks show significant difference ($P < 0.05$) from the frequency in the cecum. *P*-values from two-way ANOVA (diet × site) in $CD8^+$ intraepithelial lymphocytes were <0.0001 for diet, site; and diet × site. *P*-value from two-way ANOVA in $CD4^+$ intraepithelial lymphocytes was 0.0122 for site. *P*-values from two-way ANOVA in $CD161^+$ were 0.0050 for diet, <0.0001 for site, and 0.0125 for diet × site.

(Fig. 3B) in rats fed various dietary fibers. The distribution patterns of the $BrdU^+$ cells were quite similar for each of the diets. The cecal epithelia had more $BrdU^+$ cells than did colonic epithelia. Almost all $BrdU^+$ epithelial layer cells were located between cell positions 1 and 17. In cecum, the number of $BrdU^+$ cells in the half-crypt section was greater in GGH- and WSF-fed rats than in FF-, CE-, and SBF-fed rats (Table 1), which appeared to be related to the total number of epithelial cells in the crypt and the organ weight. No significant difference in the number of $BrdU^+$ cells among the groups was observed in the distal colonic epithelium. Two-way ANOVA analysis revealed significant differences in the number of $BrdU^+$ epithelial layer cells for diet $P < 0.0001$, site $P < 0.0001$, and diet × site $P = 0.0037$. In addition, the number of $BrdU^+$ epithelial cells in the crypt was positively correlated with epithelial cell number in the cecal crypt ($r^2 = 0.64$, $P < 0.0001$) and cecal organ weight ($r^2 = 0.69$, $P < 0.0001$).

Localization of Intraepithelial and Pericryptal Immune Cells. We further analyzed the number of the immune cells on a cell-positional basis (Fig. 4A–F) because we could discriminate proliferating epithelial region (containing almost all BrdU-incorporated cells in cell positions 1–17 from the bottom of the crypt) from the differentiated epithelial region (cell position >17), using the BrdU-incorporation data (Fig. 3). Interestingly, distribution of immune cells depended on the type of immune cell. $CD8^+$ IELs preferentially located at the differentiated cell position (>17) both in cecum (Fig. 4A) and colon (Fig. 4D). Moreover, ingestion of fermentable dietary fiber (SBF, GGH, and WSF) enhanced the accumulation of $CD8^+$ IELs in the cecum. On the contrary, a significantly large number of $CD161^+$ NK cells was located in the proliferating cell position (1–17) by ingesting fermentable fiber in the cecum (Fig. 4C), but such a difference was not observed in the distal colon (Fig. 4F). These responses were prominent in the cecal epithelium. No characteristic localization was seen in $CD4^+$ IELs (Figs. 4B and E). The number of $BrdU^+$ epithelial cells was positively correlated with the number of $CD8^+$ IELs at the cell position >17 ($r^2 = 0.40$, $P < 0.0002$) in the cecal crypt.

Figure 5 shows the relationship between number of $CD8^+$ IELs located at cell position >17 and number of $CD161^+$ NK cells located at cell positions 1–17 in the cecal epithelium of rats fed various dietary fibers. There was a significant correlation between the two ($r^2 = 0.56$, $P = 0.0001$), regardless of dietary fiber ingestion.

Concentration of Organic Acids in the Cecal Contents. Table 2 shows the concentration of organic acids in the cecal contents of rats fed various dietary fibers. From the fermentation profile, there was a characteristic organic acid production in cecal contents for each of the dietary fibers tested. Butyric acid was heavily produced in the rats fed SBF. In GGH-fed rats, the major fermentation products were acetic acid and lactic acid, whereas succinic acid and lactic acid were produced in WSF-fed rats. CE is less fermentable than other fibers in terms of the organic acid production in the cecum. Because the cecum is a major fermenter in the large intestine of rats, we analyzed the relationships between the accumulation of immune cells and the cecal organic acid concentration (Table 3). The number of $CD8^+$ IELs had a significant positive association with the concentration of lactic acid, acetic acid, and butyric acid, and a negative relation with succinic acid and isovaleric acid. The number of $CD4^+$ IELs and $CD161^+$ NK cells was negatively associated with lactic acid and succinic acid, respectively.

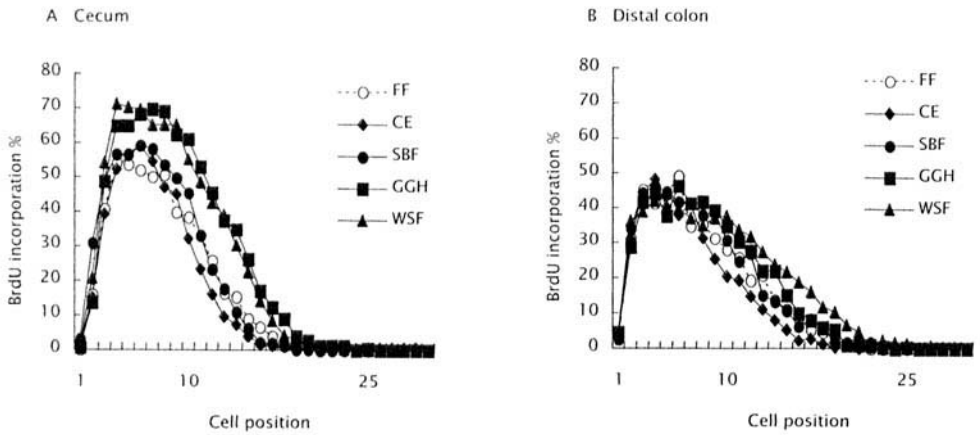

Figure 3. BrdU-incorporation of epithelial-lining cells in the cecum (A) and distal colon (B) in rats fed various dietary fibers (n = 6). Almost all $BrdU^+$ epithelial layer cells were located at the base of the crypt (cell positions 1–17), both in the cecum and colon. At cell position >17, the percentage of $BrdU^+$ cells was below 10% in each cell position.

Discussion

We demonstrated the physiological localization of $CD8^+$ IELs and $CD161^+$ NK cells along the longitudinal crypt axis of the large intestine. It is well known that proliferating epithelial cells localize to the bottom of crypts (8). The frequency with which preneoplastic cells arise from proliferating epithelial cells is considered to be much higher than that of their arising from differentiated epithelial cells. Causal relationships among inflammation, innate immunity, and cancer are widely accepted, but many of the molecular and cellular mechanisms mediating these relationships remain unknown (22). Thus, localization of immune cells around the crypt, especially of T cells and NK cells, has to be very important. Nevertheless, until now there has been no report focused on the longitudinal distribution around crypts of such immune cells.

We investigated the relationship between the localization of immune cells in pericryptal region and that of proliferating epithelial cells, because $CD8^+$ IELs appeared at a glance to locate at a relatively higher cell position from the crypt base. We found that $CD8^+$ IELs clearly exist in the epithelial lining of the crypt, whereas $CD161^+$ NK cells did not seem to locate in the intraepithelium. However, many $CD161^+$ NK cells appeared around the crypt base. Our study indicates that some of the $CD161^+$ population locates adjacent to the epithelial cells in the pericryptal region and that the isolated IEL fraction contains such periepithelial immune cells, as well as IELs.

Previous reports have shown that the isolated rat IEL fraction contains $CD3^-NKR\text{-}P1^+$ ($CD161^+$) cells (6, 7). These cells are mostly restricted to the $CD4^-CD8^-CD3^-$ population and have the ability to kill NK-sensitive targets. Some reports show the existence of NKT cells in the IEL fraction. $CD161^+$ T cells are shown to be abundant in human intestinal epithelium (22), and $CD3^+NKR\text{-}P1^+$ ($CD161^+$) cells transiently increase within a few days after infection of *Listeria monocytogenes* in rats (23). These results indicate a significance of NKT cells in the maintenance of epithelial homeostasis. However, it has also been reported that $DX5^+NK1.1^+CD4^-CD8^-$ cells in the T-cell-receptor-negative fraction of the IELs have significant cytotoxic activity in mice (24). In addition, our results showed that the $CD161^+$ NK cells were not totally identical to $CD8^+$ IELs because of the characteristic localization.

This is, however, the first report showing a spatial arrangement of IELs and NK cells along the longitudinal crypt axis. We do not exclude the possibility that some $CD161^+$ NK cells have CD8 molecules on the surface; these cells may play a role in the maintenance of epithelial homeostasis in the large intestine in pathogenic conditions. It is especially interesting to clarify the mucosal network between the cells residing at the intestine. Our study showed that $CD161^+$ NK cells located as some clusters in cecum

Table 1. Number of BrdU-Positive and Total Epithelial Cells in Cecal Half-Crypt Section and Cecal Organ Weight of Rats Fed Various Dietary Fibers[a]

	No. of $BrdU^+$ cells	No. of epithelial cells	Cecal organ weight (g)
Fiber-free	5.1 ± 0.2[b]	29.5 ± 1.1[c]	0.52 ± 0.03[b]
Cellulose	4.7 ± 0.1[b]	28.2 ± 0.7[c]	0.45 ± 0.01[b]
Sugar beet fiber	5.6 ± 0.1[b]	30.0 ± 0.7[c]	0.53 ± 0.03[b]
Guar-gum hydrolysate	7.7 ± 0.6[a]	38.9 ± 0.8[a]	1.00 ± 0.08[a]
Water-soluble soybean fiber	7.5 ± 0.3[a]	35.1 ± 0.3[b]	1.07 ± 0.05[a]

[a] Values are expressed as mean ± SEM. Values in a column with different letters are significantly different, $P < 0.05$, n = 6.

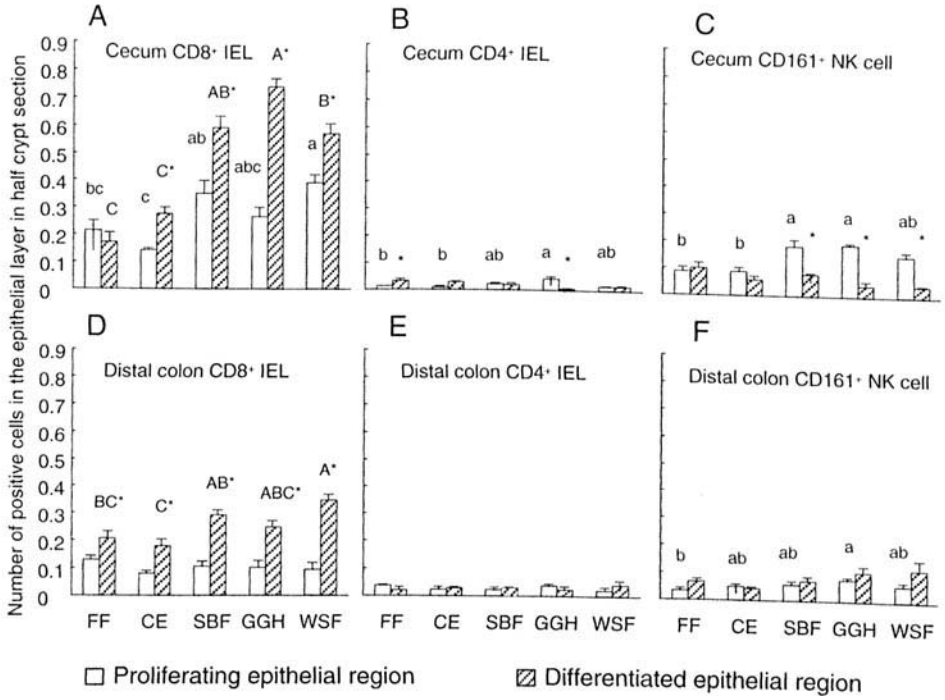

Figure 4. Number of $CD8^+$ (A, D) and $CD4^+$ (B, E) intraepithelial lymphocytes and $CD161^+$ natural killer cells (C, F) in the proliferating region (open bars) and differentiated region (slashed bars) in the crypts of the large intestine of rats fed various dietary fibers. The data were shown as the means ± SEMs (n = 6). Bars with different small letters shows significant differences ($P < 0.05$) in the proliferating cell position (1–17) among dietary groups. Bars with different capital letters show significant differences ($P < 0.05$) in differentiated cell position (>17) among dietary groups. Asterisks show significant difference ($P < 0.05$) from the number in the proliferating cell position (1–17).

(Fig. 1D) rather than as single cells in the large intestine, but their function remains unclear.

The frequency of $CD8^+$ IELs (Fig. 2A) decreased toward the distal part of the large intestine. This result is consistent with our previous report using same strain of rats (16). In humans, similar results have been observed for $CD3^+$, $CD8^+$, and $CD103^+$ IELs in the large intestine,

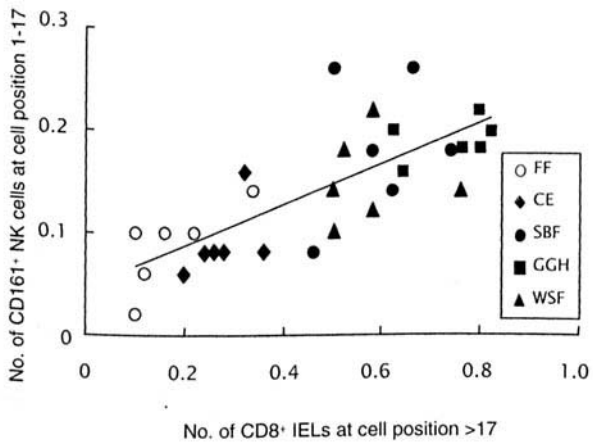

Figure 5. Relationship between the number of $CD8^+$ intraepithelial lymphocytes located at cell position >17 and the number of $CD161^+$ natural killer cells at cell positions 1–17 in the half-crypt section of the cecum of rats fed various dietary fibers. The scatter plot contains individual values from rats fed fiber-free, cellulose, sugar beet fiber, guar-gum hydrolysate, and water-soluble soybean fiber. Symbols are same as those in Figure 3. Significant regression was observed between the two ($r^2 = 0.56$, $P < 0.0001$).

although the earlier study does not confirm the longitudinal localization of these immune cells (25). It is notable that ingestion of dietary fibers potentiated such localization of the $CD8^+$ IELs and $CD161^+$ NK cells. Physiological accumulation of $CD8^+$ IELs has been enhanced in crypts of rats fed fermentable dietary fibers (SBF, GGH, and WSF), whereas the level was lower in CE-fed rats (Fig. 2A). This indicates that luminal fermentation pattern is an important factor in the characteristic localization of the immune cells. In contrast, the frequency of $CD4^+$ IELs tended to increase toward the distal large intestine but was not changed by modulating the diet.

Almost all proliferating epithelial cells were located at cell positions 1–17 of the crypt in both the cecum (Fig. 3A) and distal colon (Fig. 3B). We further analyzed the distribution of immune cells in the proliferating epithelial area at cell positions 1–17 and in the differentiated epithelial area at cell position >17. Our results indicate that a variation in distribution depends on the type of immune cells in the pericryptal region of the large intestine. The cell-positional analysis revealed evidence that all fermentable dietary fibers used in this study potentiated the frequency of $CD8^+$ IELs located among differentiated epithelial cells, whereas the $CD161^+$ NK cells were located at the bottom of the crypt. This indicates that the chemoattractant from the proliferating epithelium may be different than those from the differentiated epithelium.

The fermentation profile of the cecal contents in the rats

Table 2. Concentration of Organic Acids in the Cecal Contents of Rats Fed Various Dietary Fibers[a]

	Succinic acid	Lactic acid	Acetic acid	Propionic acid (μmol/g cecal contents)	Isobutyric acid	Butyric acid	Isovaleric acid	Valeric acid
Fiber-free	29.9 ± 4.1^{a}	1.0 ± 0.1^{b}	46.8 ± 4.5^{ab}	15.3 ± 1.3^{a}	3.4 ± 3.4	9.1 ± 1.4^{b}	1.11 ± 0.10^{a}	1.63 ± 0.21^{a}
Cellulose	14.1 ± 2.7^{bc}	0.4 ± 0.2^{b}	23.6 ± 4.8^{b}	6.2 ± 1.4^{b}	3.8 ± 3.8	7.5 ± 1.8^{b}	0.75 ± 0.17^{a}	1.01 ± 0.20^{b}
Sugar beet fiber	4.8 ± 1.8^{c}	0.1 ± 0.1^{b}	59.2 ± 1.9^{a}	11.0 ± 0.9^{ab}	4.9 ± 3.2	17.0 ± 0.8^{a}	0.27 ± 0.04^{b}	0.92 ± 0.10^{b}
Guar-gum hydrolysate	5.4 ± 3.6^{c}	10.9 ± 2.7^{a}	56.6 ± 10.7^{a}	10.7 ± 2.5^{ab}	ND	8.6 ± 2.5^{b}	ND	ND
Water-soluble soybean fiber	22.0 ± 3.8^{ab}	8.1 ± 1.6^{a}	46.4 ± 5.8^{ab}	7.2 ± 0.9^{b}	ND	9.3 ± 1.8^{b}	0.03 ± 0.03^{b}	0.03 ± 0.03^{c}

[a] Values are expressed as mean ± SEM. Values in a column with different letters are significantly different, $P < 0.05$, n = 6. ND, not detected.

varied according to the dietary fiber ingested (Table 2). In general, fermentation generates SCFAs that are known to affect the activities of the large intestine. For example, butyrate both is used as a primary energy source in colonic epithelial cells (13, 14) and stimulates normal epithelial cell proliferation (15). The dietary fibers used in this study have various cecal fermentation profiles (Table 2). We also found significant relationships between cecal concentration of organic acids and accumulation of IELs and NK cells, although the correlations were not quite strong (Table 3). Sanderson and colleagues showed a regulation of chemoattractant expression by sodium butyrate using cell culture systems (26). Of dietary fibers used in this study, SBF-fed rats had significantly larger amounts of butyrate in cecal contents than others (Table 2), and the accumulation of $CD8^+$ IELs and $CD161^+$ NK cells was promoted (Figs. 4A and C) without an increase in the epithelial proliferation (Fig. 3A) in the cecum. Intestinal epithelial cells are also known to produce a variety of chemokines on occasion (28–30).

Recently, it has been reported that butyrate modulates the production of MCP-1 and IL-8 in human intestinal epithelial cells in a different manner (26, 31). The chemoattractants and cytokines secreted from the epithelial cells may differ between proliferating and differentiated epithelial cells and may also be modulated by the ingestion of fermentable dietary fibers. These results indicate that SCFA produced from dietary fibers is one of the factors modulating localization of these IELs and NK cells. There also seems to be another factor involved, such as bacterial cell components. Naik *et al.* (27) reported that intestinal epithelial cells have Toll-like receptors for bacterial

Table 3. Relationship Between the Ratio of the Number of Cecal Intraepithelial Lymphocytes and Natural Killer Cells Against 100 Epithelial Layer Cells and Organic Acid Concentrations in the Cecal Contents of Rats Fed Various Dietary Fibers

Phenotype and organic acid	Relation[a]	r^2	*P* value
$CD8^+$			
Succinic acid	–	0.16	0.0253
Lactic acid	+	0.16	0.0273
Acetic acid	+	0.28	0.0025
Butyric acid	+	0.20	0.0145
Isovaleric acid	–	0.55	<0.0001
$CD4^+$			
Lactic acid	–	0.16	0.0302
$CD161^+$			
Succinic acid	–	0.13	0.0500

[a] Relation shows positive (+) and negative (–) relationship between the ratio of the immune cells against 100 epithelial layer cells and the organic acid concentration (n = 30). *P* values show the significance of the slope of the regression line between the number of immune cells and the concentration of certain SCFA. $P < 0.05$ is considered to be significant.

products in the luminal contents. It is possible that the bacterial cell components themselves modify the expression of a variety of IEL and NK chemoattractants in the epithelial cells.

This study showed that the accumulation of $CD8^+$ IELs in the differentiated area in the crypt was accompanied by an increase in $CD161^+$ NK cells at the bottom of the crypt (Fig. 5). SBF did not induce an increase in proliferating epithelial cells in the crypt of cecum despite their high concentration of butyrate in the contents (Fig. 3A; Tables 1 and 2), but they did promote both $CD8^+$ IEL and $CD161^+$ NK accumulation (Figs. 2 and 4). These results indicate that the proliferation of epithelial cells was not directly related to the accumulation of IELs and NK cells in the large intestine. A combination of the organic acid pattern, together with bacterial profile in the luminal contents, seems to alter the pattern of chemoattractants released from the intestinal epithelium for certain IELs or NK cells (Fig. 6).

In the bottom of the crypt there are many proliferating cells that may produce aberrant epithelial cells. Presumably, the NK cells, including NKT cells near the proliferating epithelial cells, are there to eliminate abnormal cells spontaneously produced by intestinal stem cells. However, $CD8^+$ IELs in the upper differentiated region of the epithelium are considered to have a protective function against infection, because epithelial cells are always coming into contact with luminal antigens and intestinal bacteria. Ingestion of fermentable dietary fibers seems to promote an accumulation of these IELs and NK cells according to the fermentation profiles, which influence homeostasis in the intestinal epithelium.

In conclusion, we demonstrated a spatial arrangement of $CD8^+$ IELs and $CD161^+$ NK cells along the longitudinal crypt axis in the crypts of the large intestine. Ingestion of fermentable dietary fiber, especially SBF, potentiated the accumulation of $CD8^+$ IELs and $CD161^+$ NK cells, probably via fermentation in the luminal contents.

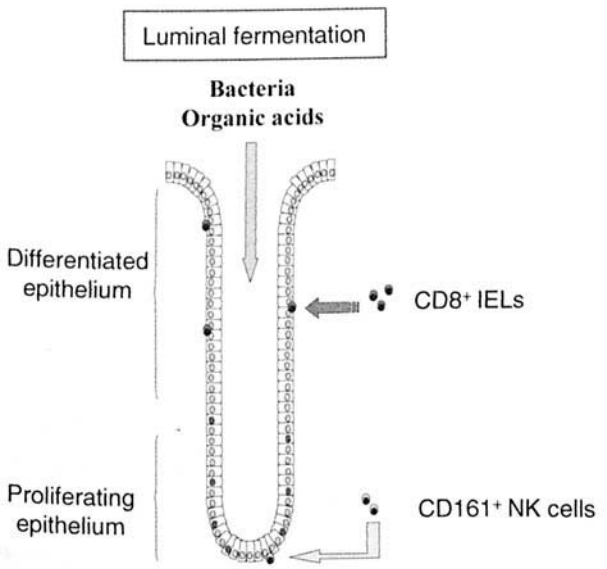

Figure 6. Differences in physiological localization of $CD8^+$ intraepithelial lymphocytes and $CD161^+$ natural killer cells along the crypt axis of the large intestine.

1. Komano H, Fujiura Y, Kawaguchi M, Matsumoto S, Hashimoto Y, Obana S, Mombaerts P, Tonegawa S, Yamamoto H, Itohara S, Nanno M, Ishikawa H. Homeostatic regulation of intestinal epithelia by intraepithelial gamma delta T cells. Proc Natl Acad Sci USA 92:6147–6151, 1995.
2. Matsuda S, Kudoh S, Katayama S. Enhanced formation of azoxymethane-induced colorectal adenocarcinoma in gammadelta T lymphocyte-deficient mice. Jpn J Cancer Res 92:880–885, 2001.
3. Bird RP. Observation and quantification of aberrant crypts in the murine colon treated with a colon carcinogen: preliminary findings. Cancer Lett 37:147–151, 1987.
4. Nagai T, Ishizuka S, Hara H, Aoyama Y. Dietary sugar beet fiber prevents the increase in aberrant crypt foci induced by gamma-irradiation in the colorectum of rats treated with an immunosuppressant. J Nutr 130:1682–1687, 2000.
5. Todd D, Singh AJ, Greiner DL, Mordes JP, Rossini AA, Bortell R. A new isolation method for rat intraepithelial lymphocytes. J Immunol Methods 224:111–127, 1999.
6. Todd DJ, Greiner DL, Rossini AA, Mordes JP, Bortell R. An atypical population of NK cells that spontaneously secrete IFN-gamma and IL-4 is present in the intraepithelial lymphoid compartment of the rat. J Immunol 167:3600–3609, 2001.
7. Brittenden J, Heys SD, Ross J, Eremin O. Natural killer cells and cancer. Cancer 77:1226–1243, 1996.
8. Potten CS. Stem cells in gastrointestinal epithelium: numbers, characteristics and death. Philos Trans R Soc Lond B Biol Sci 353:821–830, 1998.
9. Hooper LV, Midtvedt T, Gordon JI. How host-microbial interactions shape the nutrient environment of the mammalian intestine. Ann Rev Nutr 22:283–307, 2002.
10. Mysorekar IU, Lorenz RG, Gordon JI. A gnotobiotic transgenic mouse model for studying interaction between small intestinal enterocytes and intraepithelial lymphocytes. J Biol Chem 277:37811–37819, 2002.
11. Stappenbeck TS, Hooper LV, Gordon JI. Developmental regulation of intestinal angiogenesis by indigenous microbes via Paneth cells. Proc Natl Acad Sci USA 99:15451–15455, 2002.
12. Macfarlane GT, Gibson GR. Microbial aspects of the production of short-chain fatty acids in the large bowel. In: Cummings JH, Rombeau JL, Sakata T. Eds. Physiological and Clinical Aspects of Short-Chain Fatty Acids. Cambridge University Press, pp87–106, 1995.
13. Fleming SE, Fitch MD, DeVries S, Liu ML, Kight C. Nutrient utilization by cells isolated from rat jejunum, cecum and colon. J Nutr 121:869–878, 1991.
14. Roediger WE. Utilization of nutrients by isolated epithelial cells of the rat colon. Gastroenterology 83:424–429, 1982.
15. Sakata T. Stimulatory effect of short-chain fatty acids on epithelial cell proliferation in the rat intestine: a possible explanation for trophic effects of fermentable fibre, gut microbes and luminal trophic factors. Br J Nutr 58:95–103, 1987.
16. Ishizuka S, Tanaka S. Modulation of $CD8^+$ intraepithelial lymphocyte distribution by dietary fiber in the rat large intestine. Exp Biol Med 227:1017–1021, 2002.
17. Mitamura R, Hara H, Aoyama Y, Chiji H. Supplemental feeding of difructose anhydride III restores calcium absorption impaired by ovariectomy in rats. J Nutr 132:3387–3393, 2002.
18. Reeves PG, Nielsen FH, Fahey GC Jr. AIN-93 purified diets for laboratory rodents: final report of the American Institute of Nutrition ad hoc writing committee on the reformulation of the AIN-76A rodent diet. J Nutr 123:1939–1951, 1993.

19. Ishizuka S, Ito S, Kasai T, Hara H. Dietary sugar beet fiber ameliorates diarrhea as an acute gamma-radiation injury in rats. Radiat Res 154:261–267, 2000.
20. Hoshi S, Sakata T, Mikuni K, Hashimoto H, Kimura S. Galactosylsucrose and xylosylfructoside alter digestive tract size and concentrations of cecal organic acids in rats fed diets containing cholesterol and cholic acid. J Nutr 124:52–60, 1994.
21. Iiai T, Watanabe H, Suda T, Okamoto H, Abo T, Hatakeyama K. $CD161^+$ T (NT) cells exist predominantly in human intestinal epithelium as well as in liver. Clin Exp Immunol 129:92–98, 2002.
22. Coussens LM, Werb Z. Inflammation and cancer. Nature 420:860–867, 2002.
23. Hirose K, Suzuki H, Nishimura H, Mitani A, Washizu J, Matsuguchi T, Yoshikai Y. Interleukin-15 may be responsible for early activation of intestinal intraepithelial lymphocytes after oral infection with *Listeria monocytogenes* in rats. Infect Immun 66:5677–5683, 1998.
24. Kinoshita N, Hiroi T, Ohta N, Fukuyama S, Park EJ, Kiyono H. Autocrine IL-15 mediates intestinal epithelial cell death via the activation of neighboring intraepithelial NK cells. J Immunol 169:6187–6192, 2002.
25. Kirby JA, Bone M, Robertson H, Hudson M, Jones DE. The number of intraepithelial T cells decreases from ascending colon to rectum. J Clin Pathol 56:158, 2003.
26. Sanderson IR. Nutritional factors and immune functions of gut epithelium. Proc Nutr Soc 60:443–447, 2001.
27. Naik S, Kelly EJ, Meijer L, Pettersson S, Sanderson IR. Absence of Toll-like receptor 4 explains endotoxin hyporesponsiveness in human intestinal epithelium. J Pediatr Gastroenterol Nutr 32:449–453, 2001.
28. Dwinell MB, Lugering N, Eckmann L, Kagnoff MF. Regulated production of interferon-inducible T-cell chemoattractants by human intestinal epithelial cells. Gastroenterology 120:49–59, 2001.
29. Shaw SK, Hermanowski-Vosatka A, Shibahara T, McCormick BA, Parkos CA, Carlson SL, Ebert EC, Brenner MB, Madara JL. Migration of intestinal intraepithelial lymphocytes into a polarized epithelial monolayer. Am J Physiol 275:G584–591, 1998.
30. Shibahara T, Wilcox JN, Couse T, Madara JL. Characterization of epithelial chemoattractants for human intestinal intraepithelial lymphocytes. Gastroenterology 120:60–70, 2001.
31. Fusunyan RD, Quinn JJ, Fujimoto M, MacDermott RP, Sanderson IR. Butyrate switches the pattern of chemokine secretion by intestinal epithelial cells through histone acetylation. Mol Med 5:631–640, 1999.